



Computational Exploration of Antifungal plant Compounds as Inhibitors of Squalene Epoxidase in Terbinafine-Resistant *Trichophyton rubrum*

 Viknesh Sasikumar^{1*},  Gopi Uchimuthu²

¹Independent Researcher, Department of Bioinformatics, Alagappa University, India.

²Independent Researcher, Department of Bioinformatics, Alagappa University, India.

DOI: <https://doi.org/10.70333/ijeks-03-12-037>

*Corresponding Author: vikneshkumar58@gmail.com

Article Info:- Received : 11 September 2024

Accepted : 27 December 2024

Published : 30 January 2025

Abstract

Dermatophytes, a group of keratinophilic fungi, are the primary causative agents of superficial skin infections, affecting an estimated 20–25% of the global population. Among these, *Trichophyton rubrum* is the most prevalent, accounting for 60% of clinical dermatophyte infections. Current treatments rely on antifungal drugs such as terbinafine, itraconazole, and fluconazole, but the emergence of resistance, particularly due to mutations in the squalene epoxidase (SE) enzyme, poses a significant challenge. This study aimed to identify plant-derived SE inhibitors through integrated computational approaches. The SE protein structure (NCBI: OM313303.1) was modeled and validated, followed by virtual screening of 631 phytochemicals from IMPPAT database against 9 reference antifungals. Molecular docking (AutoDock Vina), ADMET profiling (SwissADME), and ligand unbinding analysis (MoMA-LigPath) were performed. Ten compounds showed superior binding ($\Delta G \leq -7.5$ kcal/mol) compared to other drugs. Among the screened compounds, IMPHY0011559 (Gibberellic acid), IMPHY005537 (Ellagic acid), IMPHY009887 (Digiferruginol), IMPHY011837 (Quinine), IMPHY004619 (Quercetin), IMPHY004388 (Kaempferol), IMPHY004038 (Eriodictyol), IMPHY002073 (Aromadendrin), IMPHY008945 (Cyanidin), and IMPHY003535 (Leucopelargonidin) exhibited favorable pharmacokinetic profiles, including optimal lipophilicity (MLOGP 1.2-3.8) and bioavailability ($\geq 80\%$). These plant-derived compounds overcome key resistance limitations by maintaining binding efficacy to mutated SE (F397L) and showing smoother unbinding pathways than antifungal drugs. Their dual advantages of strong target inhibition and favorable ADMET properties position them as possible candidates for next-generation antifungals.

Keywords: *Trichophyton rubrum*, *Squalene Epoxidase*, *Molecular docking*, *ADMET*.



2583-7354/© 2025 Viknesh Sasikumar and Gopi Uchimuthu. This is an open access article distributed under the Creative Commons Attribution License (<https://creativecommons.org/licenses/by/4.0/>), which permits unrestricted use, distribution, and reproduction in any medium, provided you give appropriate credit to the original author(s) and the source, provide a link to the Creative Commons license, and indicate if changes were made.

1. INTRODUCTION

Dermatophytes are fungi that cause an infectious skin disease. These pathogens are attracted to keratin, which is present in mammalian skin, hair, and nails. The frequency and prevalence of these superficial infections are exceedingly high, with an estimated 20 to 25% of the global population infected [3]. The fungi include *Trichophyton*, *Microsporum* and *Epidermophyton*. In terms of morph these fungi are septal hyphae molds that multiply asexually in warm settings [1]. *Trichophyton rubrum* is the most prevalent fungal dermatophyte, which is responsible for 60% of clinical dermatophyte infections. It causes persistent skin illnesses such as infections of toe nails, athlete's foot, ringworm, and jock itch [4]. Although these illnesses are not lethal, they can impair a person's quality of life by causing discomfort, psychological stress, and social embarrassment. Epidemiological studies reveal distinct patterns of cutaneous fungal infections across Asian populations. Dermatophytes account for approximately 40-48% of reported cases, representing the most prevalent causative agents. Yeast infections follow closely, comprising 43-46% of diagnoses, while nondermatophyte molds are less common, responsible for only 8-11% of skin mycoses [6]. Dermatophytes secrete numerous proteases that degrade keratinized structures into oligopeptides and free amino acids, which are subsequently utilized by the fungi as sources of nutrients. These activity also involving in pathogenesis [5]. The dermatophyte *Trichophyton rubrum*'s pathogenicity is determined by its cell wall composition. For example, mannans suppress lymphocytes, a subtilisin homolog triggers host immunological responses, and LysM proteins protect chitin and glucans from the immune system [10]. Chitin, glucans, and mannans are also a sources of pathogen-associated molecular patterns (PAMPs) that originate from the fungal cell wall. The innate immune system, which defends against fungal infections, is aware of these. Numerous cell wall-based strategies have been developed by pathogenic fungi to aid in their evasion of host immune systems [4]. Four gene classes that may be involved in the pathogenicity of dermatophytes are enriched in their genomes. Proteases that break down skin are one example; kinases, including pseudokinases, that are involved in signaling required for skin adaptation;

secondary metabolites, which are substances that function as toxins or signals in interactions between the fungus and host; and a class of proteins (LysM) that seem to bind and hide carbohydrates and cell wall components, thereby evading the host's immune response to the fungi. These genome sequences offer a solid starting point for further research into the pathogenic mechanisms [11]. The clinical management of dermatophytosis employs multiple therapeutic approaches, though each presents notable limitations. While existing antifungal regimens demonstrate satisfactory clinical efficacy, their use is constrained by two significant factors: (1) the potential for adverse effects and (2) the increasing prevalence of drug-resistant fungal strains. Among available options, azole derivatives remain a first-line treatment choice due to their triple advantage of broad antifungal activity, chemical stability, and optimal oral absorption characteristics. Contemporary antifungal agents are classified by their mechanism of action, with major categories including polyenes, azoles, allylamines, and echinocandins [6]. Acquired resistance, frequently observed in numerous fungi, continues to be a substantial issue. While "*T. rubrum*" can develop resistance to azoles, amorolfine, and terbinafine when exposed to sub-inhibitory concentrations of these drugs for extended periods of time, studies have shown that "*T. rubrum*" has a limited capacity to develop resistance to terbinafine, even after prolonged exposure [16]. A number of drug classes block the metabolism of fungi. One important component of fungal cell membranes, ergosterol, is inhibited by polyenes, which alters its function and eventually causes membrane disruption. Current antifungal therapies primarily target fungal membrane biosynthesis through two key pathways. Terbinafine exerts its effect by specifically inhibiting squalene epoxidase also known as squalene monooxygenase, a crucial enzyme in ergosterol production. This enzyme represents an attractive therapeutic target due to its essential role in maintaining fungal membrane integrity. Functioning in the endoplasmic reticulum, SM catalyzes the oxidation of squalene to (S)-2, 3-epoxysqualene using FAD and NADPH as cofactors - a rate-limiting step in fungal ergosterol biosynthesis. The enzyme contains two functionally important regions: an N-terminal FAD-binding oxidoreductase domain (residues 40-70) and a central squalene epoxidase catalytic

domain (residues 191-465). Similarly, azole-class antifungals (including ketoconazole, itraconazole, fluconazole, and voriconazole) act by blocking 14 α -lanosterol demethylase, another essential enzyme in the ergosterol synthesis pathway. Additional therapeutic targets in *T. rubrum* include chitin synthase, heat shock proteins, C-14 sterol reductase, C-8 sterol isomerase, and 1, 3- β -glucan synthase, with most antifungal classes focusing on disrupting ergosterol biosynthesis [6]. Our investigation employed a systematic review of peer-reviewed literature to identify plant species with documented antifungal properties. These findings were cataloged and presented in Table 1. Resistance patterns revealed a significant case involving amino acid substitution (F397L) in squalene epoxidase, distinct from the previously reported L393F mutation. The NFI5166 resistant isolate demonstrated cross-resistance to SE inhibitors while maintaining susceptibility to other antifungal classes. Microsomal assays confirmed reduced terbinafine sensitivity in this strain, with molecular analysis pinpointing the F397L substitution in close proximity to the L393F mutation site, suggesting a critical binding region for terbinafine [24]. Molecular docking studies evaluated interactions between both synthetic antifungals and plant-derived compounds with *T. rubrum*'s squalene epoxidase. Our computational analysis revealed detailed binding interactions, including hydrogen bonds, hydrophobic contacts, and van der Waals forces, providing mechanistic insights into the inhibitory potential of these compounds. These findings underscore the promise of plant-derived molecules as novel antifungal agents against *T. rubrum*.

Table-1: Antifungal activity Plants

| S.no | Antifungal activity Plants | Reference |
|------|----------------------------|-----------|
| 1 | Senna alata linn | [14] |
| 2 | cassia fistula | [20] |
| 3 | piper betle | [21] |
| 4 | terminallia chebula | [23] |
| 5 | Rubia tinctorum | [19] |
| 6 | Tithonia Diversifolia | [19] |
| 7 | Epilobium angustifolium | [15] |
| 8 | lawsonia inermis | [22] |
| 9 | Acalypha indica | [22] |
| 10 | lawsonia inermis | [22] |

2. MATERIALS AND METHODS

2.1 Preparation of protein and ligands

The amino acid sequence of the *T. rubrum* squalene epoxidase protein (accession number: #OM313303.1)(strain- NFI5166) was obtained from the NCBI database (<https://www.ncbi.nlm.nih.gov/>)[42]. The secondary structure of the protein was predicted using the trRosetta server (figure 1) (<https://yanglab.qd.sdu.edu.cn/trRosetta/>)[43]. The generated protein models are then evaluated using Procheck@ (<https://saves.mbi.ucla.edu/>) [44], with their structural integrity assessed through Ramachandran plots. The Ramachandran plot analysis showed that 89.5% of residues are in core regions, 9.3% in allowed regions, 0.5% in generously allowed regions, and only 0.7% in disallowed regions. This indicates a high-quality model with minimal stereochemical deviations, supporting its structural reliability. ProSA-web – Protein Structure Analysis (<https://prosa.services.came.sbg.ac.at/prosa.php>) [25]. The modelled protein was validated using the ProSA web server, obtaining a Z-score of -9, which falls within the range of experimentally determined structures. This indicates high structural reliability, making the model suitable for further computational studies. Before docking, the protein was processed using AutoDock Tools 1.5.7, where water molecules and polar hydrogens along with Kollman charges were added. The finalized structure was subsequently saved in pdbqt format [17][30].

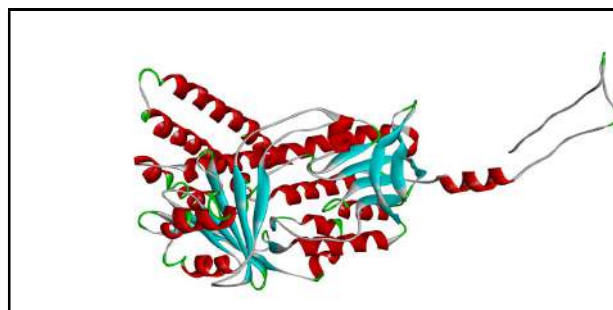


Fig-1: Predicted secondary structure of squalene monooxygenase

Nine common topical and systemic antifungal medications were taken from the PubChem database (<https://pubchem.ncbi.nlm.nih.gov/>)[45]. These include **luliconazole**, **amorolfine**,

terbinafine, itraconazole, bifonazole, ketoconazole, miconazole, fluconazole, and naftifine based on the experiment [16], while antifungal plant compounds were downloaded from the IMPPAT plant compounds database (Table 1) (<https://cb.imsc.res.in/imppat/home>) [46][47].

2.2 Screening of plant compounds

The plant-derived 631 compounds were systematically screened using the SwissADME tool (<https://www.molecular-modelling.ch/swiss-drug-design.html>) [27][49][50] to evaluate their potential as antifungal agents. The screening process was based on critical criteria, including bioavailability, drug-likeness, and compliance with Lipinski's Rule of Five. These parameters ensured that the selected compounds exhibited favorable pharmacokinetic properties and a high likelihood of therapeutic efficacy. Compounds derived from plants with known antifungal activity were prioritized, enabling the identification of

promising candidates for further investigation [27]. These compounds were subsequently prepared and optimized using Open Babel, an open-source chemical toolbox that facilitates the manipulation and conversion of chemical data. The preparation process involved the application of the steepest descent algorithm, a gradient-based optimization technique, to minimize the energy of the molecular structures. The MMFF94 (Merck Molecular Force Field 94) was utilized as the force field to accurately model the molecular interactions and energetics. Additionally, hydrogen atoms were explicitly added to the structures to ensure completeness and accuracy in the molecular representation. The optimization procedure was carried out with a specified maximum number of steps, set to the default value of 2500, to achieve a balance between computational efficiency and convergence to a stable molecular configuration [18].

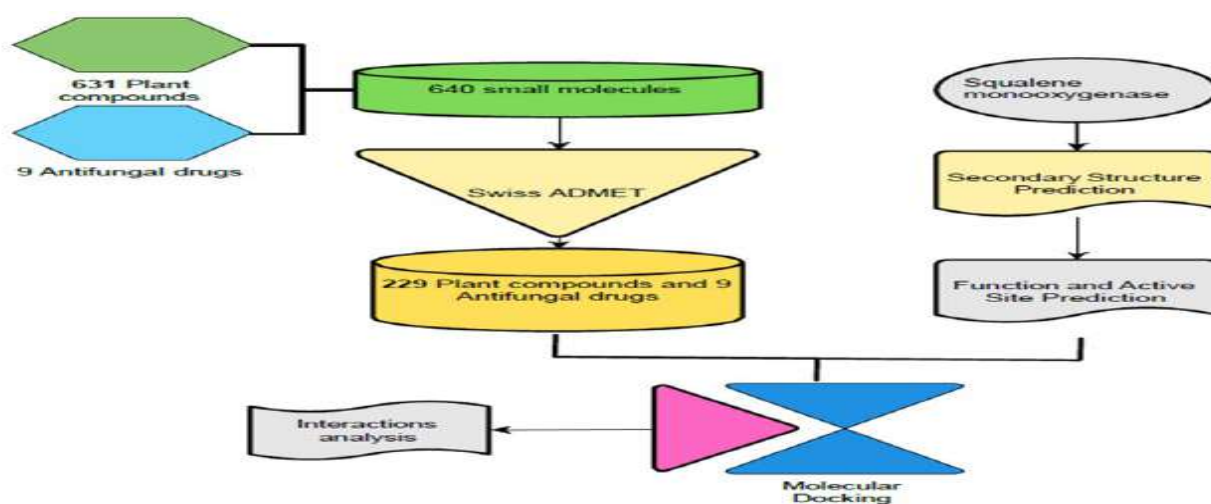


Fig-2: Process Flow Chart

2.3 Active site prediction

The active site of the protein was predicted through a combination of literature review and computational analysis using the CASTp Fold online tool (<https://cfold.bme.uic.edu/castpfold/>) [28]. Special emphasis was placed on identifying regions associated with terbinafine resistance, as these sites are critical for understanding the protein's functional and structural dynamics. Specifically, the mutated regions linked to terbinafine resistance were prioritized and

considered as potential active sites for further investigation. This approach ensured a targeted and biologically relevant analysis of the protein's functional domains [41].

2.4 Functional prediction of protein

The functional prediction analysis of the target protein sequence was performed using ProtNLM (<https://310.ai/docs/function/protnlm>) [32], a protein neural language model, to identify its potential biological role. The top prediction, with a confidence score of 0.725,

assigned the protein to the enzyme class EC 1.14.14.17, indicating it is likely a cytochrome P450 monooxygenase. Cytochrome P450 enzymes are known for their critical roles in oxidation reactions, including drug metabolism, steroid biosynthesis, and detoxification processes. This high-confidence prediction suggests that the target protein may function in similar metabolic pathways, potentially contributing to the oxidation of various substrates. A secondary prediction, with a lower confidence score of 0.266, identified the protein as a squalene monooxygenase, an enzyme involved in the biosynthesis of sterols and triterpenes by catalyzing the conversion of squalene to squalene epoxide. While this prediction is less certain, it provides an alternative hypothesis for the protein's function, particularly in sterol-related pathways. The remaining predictions, including FAD-dependent monooxygenase, SE domain-containing protein, and other oxidoreductases, were assigned significantly lower scores (≤ 0.001), indicating low confidence and likely limited relevance to the protein's primary function [32].

3. MOLECULAR DOCKING

Molecular interaction studies were conducted using AutoDock Vina to investigate the binding potential of the prepared protein with both commercially available antifungal drugs and the screened plant compounds. A total of 229 plant-derived compounds and 9 antifungal drugs were docked against the squalene epoxidase protein to gain insights into the binding interactions and mechanisms. AutoDock Vina employs an advanced optimization algorithm that combines a specialized scoring function (integrating empirical and knowledge-based approaches) with a gradient-based local search genetic algorithm. This approach ensures accurate prediction of binding modes and reliable analysis of receptor-ligand interactions. During the docking process, the protein was maintained in a rigid conformation, while the ligands were allowed to remain flexible to explore optimal binding orientations. The grid box was centered at coordinates $x = 4.621$, $y = -21.724$, and $z = -19.196$ to encompass the active site of the protein. Binding affinities were calculated for each ligand-protein complex, with more negative values indicating stronger binding interactions. Based on the docking scores, the top ten compounds from

the 229 screened were selected for further detailed interaction analysis. These compounds exhibited the highest binding affinities, suggesting their potential as promising candidates for further investigation [18].

3.1 Visualization of the interactions

The docking results were visualized and analyzed using PyMOL[50] and Discovery Studio Visualizer[31] to gain insights into the binding modes and interactions of the top 10 compounds. From virtual screening we identified several antifungal plant-derived compounds, including IMPHY0011559 (Gibberellic acid), IMPHY005537 (Ellagic acid) from *Terminalia chebula*, IMPHY009887 (Digiferruginol) from *Rubia tinctorum*, IMPHY011837 (Quinine) from *Acalypha indica*, IMPHY004619 (Quercetin) and IMPHY004388 (Kaempferol) from *Cassia fistula*, *Acalypha indica*, *Epilobium angustifolium*, *Lawsonia inermis*, and *Senna alata*, IMPHY004038 (Eriodictyol) from *Epilobium angustifolium*, IMPHY002073 (Aromadendrin) from *Cassia fistula*, IMPHY008945 (Cyanidin) from *Lawsonia inermis*, and IMPHY003535 (Leucopelargonidin) from *Cassia fistula*. The docking affinity (binding energy) and interacting residues of the top 10 compounds from the screened library, along with the reference antifungal drugs, is summarized in Table 2 and figure 7. These results provide a comparative assessment of the binding strengths and highlight the most promising candidates for further investigation[30][31].

IMPHY011559 has an interaction energy of -8.7 kcal/mol, stabilized by hydrogen bonds with GLU A:83 and THR A:336, including a carbon-hydrogen bond. Pi-alkyl interactions occur with PHE A:415, PHE A:412, and VAL A:237, while alkyl bonds involve LEU A:427, LEU A:335, LEU A:397, LEU A:393, and VAL A:237. **IMPHY011837** shows a binding energy of -8.3 kcal/mol, featuring a pi-sigma interaction with PHE A:123 and pi-alkyl interactions with PHE A:123, TYR A:110, LEU A:426, VAL A:112, VAL A:237, LEU A:393, PRO A:244, LEU A:335, LEU A:397, and TYR A:397. An alkyl bond with PRO A:84 and a pi-pi T-shaped interaction with PHE A:415 further stabilize the complex. **IMPHY004619** has a binding energy of -7.9 kcal/mol, with a hydrogen bond to TYR A:248 and pi-alkyl interactions with LEU A:426 and LEU A:427. A pi-pi stacked interaction with PHE A:123

also contributes to stability. **IMPHY009887** exhibits a binding energy of -8.0 kcal/mol, supported by two hydrogen bonds with TYR A:248 and pi-alkyl interactions with VAL A:237, VAL A:112, and LEU A:427. **IMPHY005537** has a binding energy of -7.9 kcal/mol, stabilized by hydrogen bonds with TYR A:394, GLN A:391 (two bonds), SER A:217, LYS A:216, and ASN A:264, along with pi-sigma and pi-alkyl interactions involving PRO A:262. **IMPHY004388** shows a binding energy of -7.8 kcal/mol, with hydrogen bonds to GLN A:83 and TYR A:248, pi-alkyl interactions with LEU A:427 and LEU A:426, and a pi-pi stacked interaction with PHE A:123. **IMPHY004038** has a binding energy of -7.7 kcal/mol, stabilized by two hydrogen bonds with TYR A:248 and one with SER A:428, along with pi-alkyl interactions involving LEU A:427 and LEU A:426, and interactions with PHE A:123. **IMPHY002073** exhibits a binding energy of -7.7 kcal/mol, featuring a hydrogen bond with TYR A:248 and pi-alkyl interactions with LEU A:426 and LEU A:427. **IMPHY008945** has a binding energy of -7.5 kcal/mol, with a hydrogen bond to GLN A:83, pi-alkyl interactions with LEU A:427

(three instances) and LEU A:426, and an unfavorable donor-donor interaction with SER A:428. **IMPHY003535** shows a binding energy of -7.5 kcal/mol, stabilized by hydrogen bonds with TYR A:394, TYR A:248 (two bonds), and GLN A:83, along with a pi-alkyl interaction with LEU A:427 and a pi-pi stacked interaction with PHE A:123. These interactions collectively contribute to the binding stability of each compound.

These compounds exhibited superior ADMET properties and docking scores compared to other compounds and reference antifungal drugs. Top 3 plant compounds and Terbinafine interactions with target protein molecule illustrated on figures (3,4,5,6). Naturally possessing antioxidant and antibiotic properties, they represent promising candidates for antifungal drug development. Their natural origin and inherent bioactivity highlight their potential as safer and more sustainable alternatives to synthetic antifungal agents, warranting further experimental validation to confirm their therapeutic efficacy and safety.

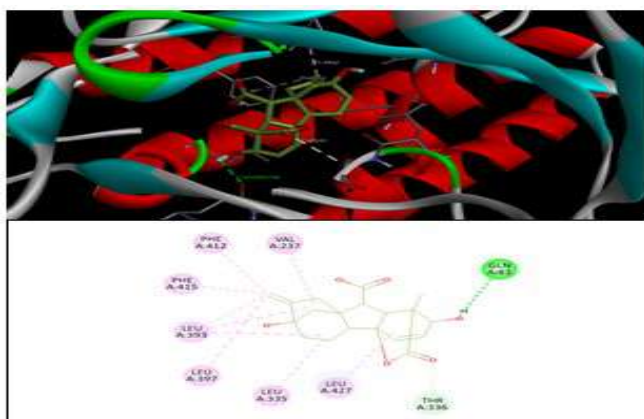


Fig-3: squalene epoxidase with IMPHY011559.

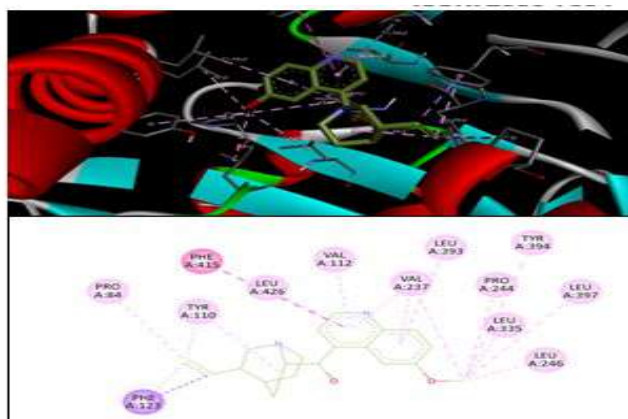


Fig-5: squalene epoxidase with IMPHY011837.

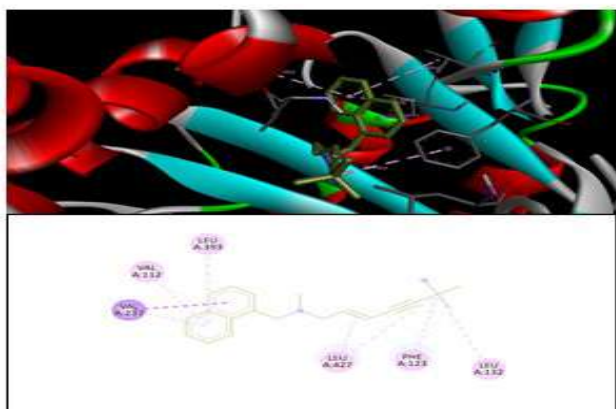


Fig-4: Squalene epoxidase with Terbinafine.

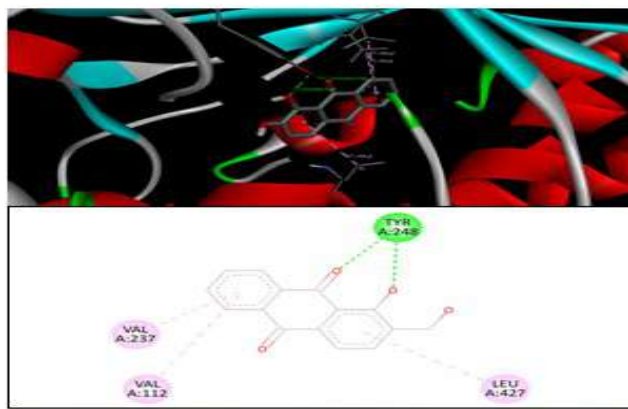


Fig-6: squalene epoxidase with IMPHY009887.

3.2 Protein-Ligand unbinding analysis

Computational analysis of the ligand-protein complex provided valuable insights into the ligand's binding and exit mechanisms, as well as its potential as an inhibitor. The docking score of the IMPHY011559 compound, at -8.7 kcal/mol, indicates strong binding affinity, reflecting stable and favorable interactions with the protein's active site. This score is comparable to or exceeds those of known inhibitors, underscoring the ligand's potential as a promising candidate for further development. MoMA-LigPath analysis ([accessible at https://moma.laas.fr/](https://moma.laas.fr/)) of the exit pathway revealed that IMPHY011559 exhibited a smoother trajectory with 137 conformations and no significant collisions. In contrast, terbinafine's pathway involved 125 conformations and encountered steric clashes with residues ARG:A-88 and ASP:A-129. The plant compound formed stable interactions with key residues ASN:A-264 and GLN:A-391, emphasizing its potential for effective inhibition. Terbinafine, while interacting with residues TYR:A-248, SER:A-428, and GLN:A-83, experienced steric hindrance, which could compromise its binding stability. These findings suggest that the novel compound holds significant promise as a potential inhibitor, with notable advantages in binding stability and release kinetics [29].

4. ADMET

The molecular weight (MW) of a substance is computed by adding the atomic masses of all its atoms and is an important aspect in medication design. Compounds should have MW values less than 500 g/mol to provide good pharmacokinetic characteristics. Hydrogen bond donors (HBD) and acceptors (HBA) are the number of hydrogen atoms that can contribute hydrogen bonds and the number of atoms that can accept them (such as oxygen or nitrogen). Compounds with less than 5 HBDs and 10 HBAs are often favoured due to their higher membrane permeability and oral bioavailability. The topological polar surface area (TPSA), which calculates the surface area of polar atoms in a molecule, is an important predictor of drugs absorption. Compounds with TPSA values less than 140 \AA^2 are commonly connected to increased bioavailability. The Moriguchi logP (MLOGP), lipophilicity metric, describes how a molecule partitions between octanol and water. Optimal drug-like compounds typically have

MLOGP values ranging from -2 to 5, which balance solubility and permeability. Bioavailability is the percentage of a medication that enters systemic circulation after delivery. It is determined by characteristics such as solubility, permeability, and metabolic stability, with higher bioavailability indicating greater therapeutic efficacy. Similarly, gastrointestinal (GI) absorption measures how well a substance is absorbed throughout the GI tract. High GI absorption is critical for attaining effective systemic concentrations after oral delivery, making it an important factor in medication development [27].

Based on the SwissADME property analysis of IMPPAT compounds derived from antifungal activity plants, numerous compounds successfully met multiple criteria for drug-likeness and ADMET properties. After rigorous screening, the top 10 compounds exhibited superior ADMET properties compared to the reference antifungal drugs. These compounds demonstrated better absorption, distribution, metabolism, excretion, and toxicity profiles, suggesting they may have fewer side effects and improved bioavailability. Furthermore, in the mutated region of the target protein, the plant compounds formed more hydrogen bond interactions, indicating stronger and more stable binding. These findings underscore the potential of these plant-derived compounds as effective and safer alternatives to conventional antifungal treatments. The physicochemical properties and pharmacokinetic parameters of the screened compounds, along with reference drugs, are detailed in Table 3.

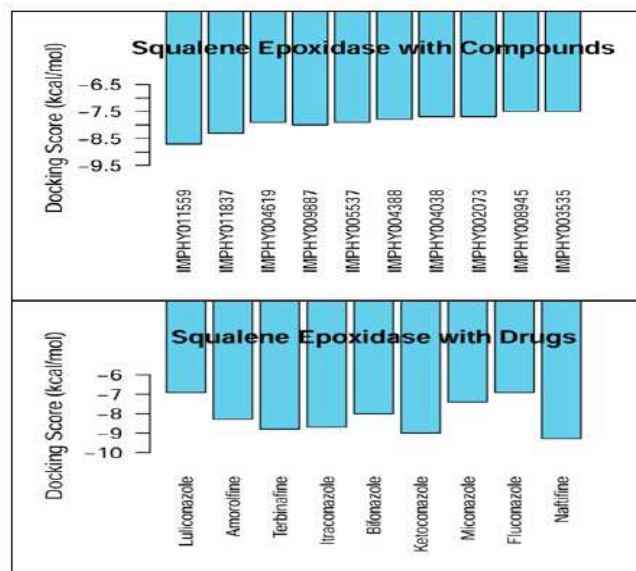
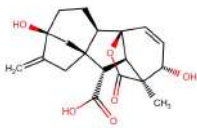
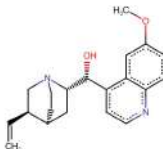
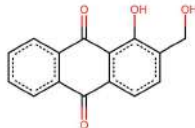
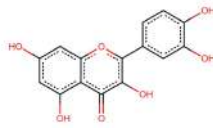
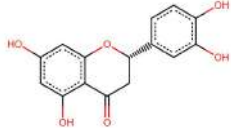
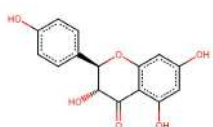
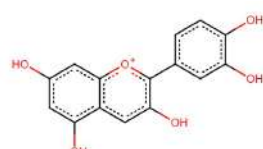
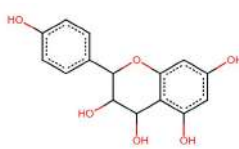


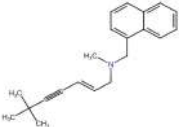
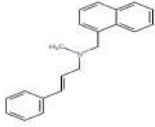
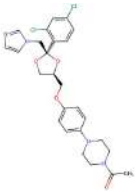
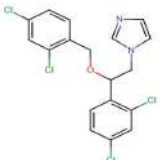
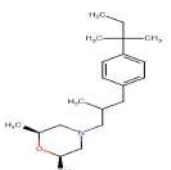
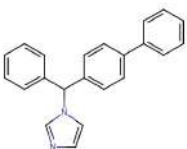
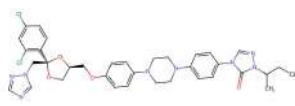
Fig-7: Docking result of Squalene epoxidase with Antifungal drugs and plant compounds

Table-2: Docking scores and interacting residues

| S.no | Ligands | Binding affinity Kcal/mol | Amino acid residues involved (discovery studio visualizer) | | | | |
|------|--------------|---------------------------|--|------------|--|---|------------------------------------|
| | | | H-bond | Pi sigma | Pi alkyl | Alkyl | Others |
| 1 | Luliconazole | -6.9 | LEU A:427, SER A:428 | - | PHE A:412, VAL A:112 | LEU A:426 | PHE A:415(pi-pinT-shaped) |
| 2 | Amorolfine | -8.3 | - | PHE A:415 | VAL A:237, PHE A:412, LEU A:393, LEU A:397, LEU A:426, LEU A:335, LEU A:427(3), | LEU A:132(2), PRO A:84 | - |
| 3 | Terbinafine | -8.8 | - | VAL A:237 | PHE A:123, VAL A:237, VAL A:112, LEU A:393 | LEU A:132, LEU A:427 | - |
| 4 | Itraconazole | -8.7 | GLN A:391, HIS A:452 | THR A:474, | VAL A:478, ILE A:388, ALA A:399, PRO A:262 | VAL A:478 | ARG A:313(pi-cation) |
| 5 | Bifonazole | -8.0 | ARG A:313, ASN A:387(pi-Donar Hydrogen bond) | VAL A:471 | ALA A:392, ALA A:448, ILE A:388, VAL A:478 | - | ARG A:313(pi-cation) |
| 6 | Ketoconazole | -9.0 | ASN A:345 | THR A:336 | LEU A:132, PRO A:84, LEU A:335, LEU A:393, LEU A:426, PHE A:412, VAL A:112 | LEU A:426 | PHE A:415(pi-pi T-shaped) |
| 7 | Miconazole | -7.4 | GLN A:83 | LEU A:426 | PHE A:412, LEU A:427, LEU A:335 | VAL A:112, VAL A:237, LEU A:132, PRO A:84 | PHE A:415(pi-pi T-shaped) |
| 8 | Fluconazole | -6.9 | TYR A:248 | LEU A:393 | LEU A:426, LEU A:246, VAL A:237 | - | TYR A:110(Halogen) |
| 9 | Naftifine | -9.3 | - | LEU A:393 | VAL A:237, VAL A:112, LEU A:427, PHE A:123, LEU A:132 | LEU A:427 | PHE A:415(pi-pi stacked) |
| 10 | IMPHY011559 | -8.7 | GLU A:83, THR A:336 (carbon hydrogen bond) | - | PHE A:415, PHE A:412, VAL A:237 | LEU A:427, LEU A:335, LEU A:397, LEU A:393, VAL A:237 | - |
| 11 | IMPHY011837 | -8.3 | - | PHE A:123 | PHE A:123, TYR A:110, LEU A:426, VAL A:112, VAL A:237, LEU A:393, PRO A:244, LEU A:335, LEU A:397, TYR A:397 | PRO A:84, | PHE A:415(pi-pi T shaped) |
| 12 | IMPHY009887 | -8.0 | TYR A:248 (2) | - | VAL A:237, VAL A:112, LEU A:427 | - | - |
| 13 | IMPHY004619 | -7.9 | TYR A:248 | - | LEU A:426, LEU A:427 | - | PHE A:123(pi-pi stacked) |
| 14 | IMPHY005537 | -7.9 | TYR A:394, GLN A:391(2),SER A:217, LYS A:216, ASN A:264 | PRO A:262 | PRO A:262 | - | - |
| 15 | IMPHY004388 | -7.8 | GLN A:83, TYR A:248 | - | LEU A:427, LEU A:426 | - | PHE A:123(pi-pi stacked) |
| 16 | IMPHY004038 | -7.7 | TYR A:248(2), SER A:428 | - | LEU A:427, LEU A:426 | - | PHE A:123 |
| 17 | IMPHY002073 | -7.7 | TYR A:248 | - | LEU A:426, LEU A:427 | - | - |
| 18 | IMPHY008945 | -7.5 | GLN A:83 | - | LEU A:427(3), LEU A:426 | - | SER A:428(unfavourabe donar-donar) |
| 19 | IMPHY003535 | -7.5 | TYR A:394, TYR A:248(2), GLN A:83 | - | LEU A:427 | - | PHE A:123(pi-pi stacked) |

Table-3: ADMET properties drugs and compounds

| COMPOUND | MW | HBD | HBA | TPSA | MLOGP | Bioavailability | GI absorption |
|--|--------|-----|-----|--------|-------|-----------------|---------------|
|  IMPHY0011559 | 346.37 | 3 | 6 | 104.06 | 1.66 | 0.56 | High |
|  IMPHY011837 | 324.42 | 1 | 4 | 45.59 | 2.23 | 0.55 | High |
|  IMPHY009887 | 254.24 | 2 | 4 | 74.6 | 0.66 | 0.55 | High |
|  IMPHY004619 | 302.24 | 5 | 7 | 131.36 | -0.56 | 0.55 | High |
|  IMPHY005537 | 302.19 | 4 | 8 | 141.34 | 0.14 | 0.55 | High |
|  IMPHY004388 | 286.24 | 4 | 6 | 111.13 | -0.03 | 0.55 | High |
|  IMPHY004038 | 288.25 | 4 | 6 | 107.22 | 0.16 | 0.55 | High |
|  IMPHY002073 | 288.25 | 4 | 6 | 107.22 | -0.1 | 0.55 | High |
|  IMPHY008945 | 287.24 | 5 | 6 | 114.29 | 0.32 | 0.55 | High |
|  IMPHY003535 | 290.27 | 5 | 6 | 110.38 | -0.02 | 0.55 | High |

| COMPOUND | MW | HBD | HBA | TPSA | MLOGP | Bioavailability | GI absorption |
|--|--------|-----|-----|-------|-------|-----------------|---------------|
|  Terbinafine | 291.43 | 0 | 1 | 3.24 | 4.89 | 0.55 | High |
|  Naftifine | 287.4 | 0 | 1 | 3.24 | 4.74 | 0.55 | High |
|  Luliconazole | 354.28 | 0 | 2 | 92.21 | 2.47 | 0.55 | High |
|  Ketoconazole | 531.43 | 0 | 5 | 69.06 | 2.47 | 0.55 | High |
|  Miconazole | 416.13 | 0 | 2 | 27.05 | 4.31 | 0.55 | High |
|  Fluconazole | 306.27 | 1 | 7 | 81.65 | 1.47 | 0.55 | High |
|  Amorolfine | 317.51 | 0 | 2 | 12.47 | 3.95 | 0.55 | High |
|  Bifonazole | 310.39 | 0 | 1 | 17.82 | 3.9 | 0.55 | High |
|  Itraconazole | 705.63 | 0 | 7 | 104.7 | 4.21 | 0.17 | High |

5. CONCLUSIONS

Dermatophytes, particularly *Trichophyton rubrum*, are among the most common fungal pathogens causing skin infections worldwide, with an estimated 20-25% of the global population affected. While these infections are generally not fatal, they significantly reduce quality of life by causing physical pain, emotional distress, and social stigma. Dermatophytes thrive by breaking down keratin, a protein found in skin, hair, and nails, using specialized enzymes called proteases. Additionally, their cell wall components, such as chitin, glucans, and mannans, help them evade the host's immune system. Research into their genomes has revealed important gene families, including proteases, kinases, secondary metabolites, and LysM proteins, which are crucial for their survival and ability to infect hosts. Squalene epoxidase (SE), a key enzyme in *Trichophyton rubrum*, plays a critical role in ergosterol biosynthesis and virulence. While terbinafine is a well-known inhibitor of SE, mutations such as F397L have led to resistance against this drug. Current antifungal treatments, such as azoles, polyenes, and allylamines, target essential fungal pathways like ergosterol biosynthesis. However, the emergence of resistance, particularly in *T. rubrum*, has become a major challenge. Resistance mechanisms, such as amino acid substitutions in the squalene epoxidase (SE) enzyme, highlight the need for novel antifungal agents with unique mechanisms of action. This study explored the potential of plant-derived compounds as alternative antifungal agents, leveraging their natural bioactivity and reduced risk of resistance development.

Molecular docking studies demonstrated that several plant-derived compounds exhibit strong binding affinities to the SE enzyme, with interaction energies comparable to or better than those of conventional antifungal drugs. Compounds such as IMPHY011559 showed superior binding stability, favorable ADMET properties, and smoother exit pathways, indicating their potential as effective inhibitors of *T. rubrum*. These findings highlight the possibilities of plant-based compounds as sustainable and safer alternatives to synthetic antifungal drugs. Furthermore, SwissADME analysis identified the top 10 plant-derived compounds with excellent drug-likeness and ADMET profiles compared to reference antifungal drugs. These compounds,

including IMPHY0011559 (Gibberellic acid), IMPHY005537 (Ellagic acid), and IMPHY011837 (Quinine), exhibited strong antifungal activity, favorable pharmacokinetic properties, and low toxicity. Their natural origin, combined with inherent antimicrobial and therapeutic properties, makes them promising candidates for addressing the growing challenge of antifungal resistance.

To conclude, this study highlights the pressing need for novel antifungal approaches to tackle dermatophytosis, especially in the context of growing resistance to existing treatments. Compounds derived from plants, with their unique mechanisms of action, favorable pharmacokinetic profiles, and minimal toxicity, show great potential as the foundation for next-generation antifungal drugs. However, their efficacy and safety must be rigorously tested through further experimental and clinical research before they can be adopted into standard dermatological practice. These natural compounds might be good not only for overcoming the limitations of current treatments but also for contributing to the global shift toward more sustainable and safer medical options. These results suggest that the identified plant compounds hold significant promise for future research and development as potential treatments for fungal skin diseases, offering a viable alternative to overcome resistance issues associated with current therapies.

ACKNOWLEDGEMENTS

The authors would like to thank all our staff and research scholars for their helpful discussions and feedback on this work.

CONTRIBUTIONS

The first author was the lead researcher and completed the data analysis. The second author shared in drafting the article and reviewing the data analysis. The authors read and approved the final manuscript.

ETHICS DECLARATIONS

The authors declare that they have no conflict of interest.

REFERENCES

- [1]. Dalei, S. R., Nayak, D., Bhue, P. K., Das, N. R., & Behera, B. (2023). [Current Status of Dermatophytosis: A Hospital-Based Study in](#)

- Northern Odisha, India. *Cureus*, 15(11), e48664. <https://doi.org/10.7759/cureus.48664>
- [2]. Cornet, L., D'hooge, E., Magain, N., Stubbe, D., Packeu, A., Baurain, D., & Becker, P. (2021). The taxonomy of the *Trichophyton rubrum* complex: a phylogenomic approach. *Microbial genomics*, 7(11), 000707. <https://doi.org/10.1099/mgen.0.000707>
- [3]. Su, H., Packeu, A., Ahmed, S. A., Al-Hatmi, A. M. S., Blechert, O., İlkit, M., Hagen, F., Gräser, Y., Liu, W., Deng, S., Hendrickx, M., Xu, J., Zhu, M., & de Hoog, S. (2019). Species Distinction in the *Trichophyton rubrum* Complex. *Journal of clinical microbiology*, 57(9), e00352-19. <https://doi.org/10.1128/JCM.00352-19>
- [4]. Kar, B., Patel, P., & Free, S. J. (2019). *Trichophyton rubrum* LysM proteins bind to fungal cell wall chitin and to the N-linked oligosaccharides present on human skin glycoproteins. *PLoS one*, 14(4), e0215034. <https://doi.org/10.1371/journal.pone.0215034>
- [5]. Ciesielska, A., Kawa, A., Kanarek, K., Soboń, A., & Szweczyk, R. (2021). Metabolomic analysis of *Trichophyton rubrum* and *Microsporum canis* during keratin degradation. *Scientific reports*, 11(1), 3959. <https://doi.org/10.1038/s41598-021-83632-z>
- [6]. Keshwania, P., Kaur, N., Chauhan, J., Sharma, G., Afzal, O., Alfawaz Altamimi, A. S., & Almalki, W. H. (2023). Superficial Dermatophytosis across the World's Populations: Potential Benefits from Nanocarrier-Based Therapies and Rising Challenges. *ACS omega*, 8(35), 31575–31599. <https://doi.org/10.1021/acsomega.3c01988>
- [7]. Zaias, N., & Rebell, G. (2004). The successful treatment of *Trichophyton rubrum* nail bed (distal subungual) onychomycosis with intermittent pulse-dosed terbinafine. *Archives of dermatology*, 140(6), 691–695. <https://doi.org/10.1001/archderm.140.6.691>
- [8]. Brescini, L., Fioriti, S., Morroni, G., & Barchiesi, F. (2021). Antifungal Combinations in Dermatophytes. *Journal of fungi (Basel, Switzerland)*, 7(9), 727. <https://doi.org/10.3390/jof7090727>
- [9]. Oguiza, J. A. (2022). LysM proteins in mammalian fungal pathogens. *Fungal Biology Reviews*, 40, 114–122. <https://doi.org/10.1016/j.fbr.2022.02.001>
- [10]. Martins, M. P., Silva, L. G., Rossi, A., Sanches, P. R., Souza, L. D. R., & Martinez-Rossi, N. M. (2019). Global Analysis of Cell Wall Genes Revealed Putative Virulence Factors in the Dermatophyte *Trichophyton rubrum*. *Frontiers in microbiology*, 10, 2168. <https://doi.org/10.3389/fmicb.2019.02168>
- [11]. Martinez, D. A., Oliver, B. G., Gräser, Y., Goldberg, J. M., Li, W., Martinez-Rossi, N. M., Monod, M., Shelest, E., Barton, R. C., Birch, E., Brakhage, A. A., Chen, Z., Gurr, S. J., Heiman, D., Heitman, J., Kosti, I., Rossi, A., Saif, S., Samalova, M., Saunders, C. W., ... White, T. C. (2012). Comparative genome analysis of *Trichophyton rubrum* and related dermatophytes reveals candidate genes involved in infection. *mBio*, 3(5), e00259-12. <https://doi.org/10.1128/mBio.00259-12>
- [12]. Ghelardi, E., Celandroni, F., Gueye, S. A., Salvetti, S., Senesi, S., Bulgheroni, A., & Mailland, F. (2014). Potential of Ergosterol synthesis inhibitors to cause resistance or cross-resistance in *Trichophyton rubrum*. *Antimicrobial agents and chemotherapy*, 58(5), 2825–2829. <https://doi.org/10.1128/AAC.02382-13>
- [13]. Ryder N. S. (1992). Terbinafine: mode of action and properties of the squalene epoxidase inhibition. *The British journal of dermatology*, 126 Suppl 39, 2–7. <https://doi.org/10.1111/j.1365-2133.1992.tb00001.x>
- [14]. Sule, W. F., Okonko, I. O., Omo-Ogun, S., Nwanze, J. C., Ojezele, M. O., Ojezele, O. J., ... & Olaonipekun, T. O. (2011). Phytochemical properties and in-vitro antifungal activity of *Senna alata* Linn. crude stem bark extract. *J Med Plants Res*, 5(2), 176–183. <https://doi.org/10.5897/JMPR.9001002>
- [15]. Webster, D., Taschereau, P., Belland, R. J., Sand, C., & Rennie, R. P. (2008). Antifungal activity of medicinal plant extracts; preliminary screening studies. *Journal of ethnopharmacology*, 115(1), 140–146. <https://doi.org/10.1016/j.jep.2007.09.014>
- [16]. Jiang, Y., Luo, W., Verweij, P. E., Song, Y., Zhang, B., Shang, Z., Al-Hatmi, A. M. S., Ahmed, S. A., Wan, Z., Li, R., & de Hoog, G. S. (2021). Regional Differences in Antifungal Susceptibility of the Prevalent Dermatophyte *Trichophyton rubrum*. *Mycopathologia*, 186(1), 53–70. <https://doi.org/10.1007/s11046-020-00515-z>
- [17]. Morris, G. M., Huey, R., Lindstrom, W., Sanner, M. F., Belew, R. K., Goodsell, D. S., & Olson, A. J. (2009). AutoDock4 and AutoDockTools4: Automated docking with selective receptor flexibility. *Journal of computational chemistry*, 30(16), 2785–2791. <https://doi.org/10.1002/jcc.21256>
- [18]. K, D., & Venugopal, S. (2024). Molecular docking and molecular dynamic simulation studies to identify potential terpenes against Internalin A protein of *Listeria monocytogenes*. *Frontiers in bioinformatics*, 4, 1463750. <https://doi.org/10.3389/fbinf.2024.1463750>

- [19]. Kaur, N., Bains, A., Kaushik, R., Dhull, S. B., Melinda, F., & Chawla, P. (2021). A Review on Antifungal Efficiency of Plant Extracts Entrenched Polysaccharide-Based Nanohydrogels. *Nutrients*, 13(6), 2055. <https://doi.org/10.3390/nu13062055>
- [20]. Sony, P., Kalyani, M., Jeyakumari, D., Kannan, I., & Sukumar, R. G. (2018). In vitro antifungal activity of cassia fistula extracts against fluconazole resistant strains of Candida species from HIV patients. *Journal de mycologie medicale*, 28(1), 193–200. <https://doi.org/10.1016/j.mycmed.2017.07.010>
- [21]. Ali, I., Khan, F. G., Suri, K. A., Gupta, B. D., Satti, N. K., Dutt, P., Afrin, F., Qazi, G. N., & Khan, I. A. (2010). In vitro antifungal activity of hydroxychavicol isolated from Piper betle L. *Annals of clinical microbiology and antimicrobials*, 9, 7. <https://doi.org/10.1186/1476-0711-9-7>
- [22]. Abirami, S., Edwin Raj, B., Soundarya, T., Kannan, M., Sugapriya, D., Al-Dayyan, N., & Ahmed Mohammed, A. (2021). Exploring antifungal activities of acetone extract of selected Indian medicinal plants against human dermal fungal pathogens. *Saudi journal of biological sciences*, 28(4), 2180–2187. <https://doi.org/10.1016/j.sjbs.2021.01.046>
- [23]. Vonshak, A., Barazani, O., Sathiyamoorthy, P., Shalev, R., Vardy, D., & Golan-Goldhirsh, A. (2003). Screening South Indian medicinal plants for antifungal activity against cutaneous pathogens. *Phytotherapy research : PTR*, 17(9), 1123–1125. <https://doi.org/10.1002/ptr.1399>
- [24]. Osborne, C. S., Leitner, I., Hofbauer, B., Fielding, C. A., Favre, B., & Ryder, N. S. (2006). Biological, biochemical, and molecular characterization of a new clinical *Trichophyton rubrum* isolate resistant to terbinafine. *Antimicrobial agents and chemotherapy*, 50(6), 2234–2236. <https://doi.org/10.1128/AAC.01600-05>
- [25]. Wiederstein, M., & Sippl, M. J. (2007). ProSA-web: interactive web service for the recognition of errors in three-dimensional structures of proteins. *Nucleic acids research*, 35(Web Server issue), W407–W410. <https://doi.org/10.1093/nar/gkm290>
- [26]. Sippl M. J. (1993). Recognition of errors in three-dimensional structures of proteins. *Proteins*, 17(4), 355–362. <https://doi.org/10.1002/prot.340170404>
- [27]. Daina, A., Michielin, O., & Zoete, V. (2017). SwissADME: a free web tool to evaluate pharmacokinetics, drug-likeness and medicinal chemistry friendliness of small molecules. *Scientific reports*, 7, 42717. <https://doi.org/10.1038/srep42717>
- [28]. Ye, B., Tian, W., Wang, B., & Liang, J. (2024). CASTpFold: Computed Atlas of Surface Topography of the universe of protein Folds. *Nucleic acids research*, 52(W1), W194–W199. <https://doi.org/10.1093/nar/gkae415>
- [29]. Devaurs, D., Bouard, L., Vaisset, M., Zanon, C., Al-Bluwi, I., Iehl, R., Siméon, T., & Cortés, J. (2013). MoMA-LigPath: a web server to simulate protein-ligand unbinding. *Nucleic acids research*, 41(Web Server issue), W297–W302. <https://doi.org/10.1093/nar/gkt380>
- [30]. Seeliger, D., & de Groot, B. L. (2010). Ligand docking and binding site analysis with PyMOL and Autodock/Vina. *Journal of computer-aided molecular design*, 24(5), 417–422. <https://doi.org/10.1007/s10822-010-9352-6>
- [31]. Biovia, D. S. (2019). Discovery Studio Visualizer. San Diego.-References.
- [32]. Gane, A., Bileschi, M. L., Dohan, D., Speretta, E., Héliou, A., Meng-Papaxanthos, L., ... & Colwell, L. J. (2022). ProtNLM: model-based natural language protein annotation. Preprint.
- [33]. Toner, P., Nelson, D., Rao, J. R., Ennis, M., Moore, J. E., & Schock, B. (2021). Antimicrobial properties of phytohormone (gibberellins) against phytopathogens and clinical pathogens. *Access microbiology*, 3(10), 000278. <https://doi.org/10.1099/acmi.0.000278>
- [34]. Sampaio, A. D. G., Gontijo, A. V. L., Lima, G. M. G., de Oliveira, M. A. C., Lepesqueur, L. S. S., & Koga-Ito, C. Y. (2021). Ellagic Acid-Cyclodextrin Complexes for the Treatment of Oral Candidiasis. *Molecules (Basel, Switzerland)*, 26(2), 505. <https://doi.org/10.3390/molecules26020505>
- [35]. Leanse, L. G., Goh, X. S., & Dai, T. (2020). Quinine Improves the Fungicidal Effects of Antimicrobial Blue Light: Implications for the Treatment of Cutaneous Candidiasis. *Lasers in surgery and medicine*, 52(6), 569–575. <https://doi.org/10.1002/lsm.23180>
- [36]. Gao, M., Wang, H., & Zhu, L. (2016). Quercetin Assists Fluconazole to Inhibit Biofilm Formations of Fluconazole-Resistant *Candida Albicans* in In Vitro and In Vivo Antifungal Managements of Vulvovaginal Candidiasis. *Cellular physiology and biochemistry : international journal of experimental cellular physiology, biochemistry, and pharmacology*, 40(3-4), 727–742. <https://doi.org/10.1159/000453134>
- [37]. Deng, Z., Hassan, S., Rafiq, M., Li, H., He, Y., Cai, Y., Kang, X., Liu, Z., & Yan, T. (2020). Pharmacological Activity of Eriodictyol: The Major Natural Polyphenolic Flavanone. Evidence-based

- complementary and alternative medicine : eCAM, 2020, 6681352. <https://doi.org/10.1155/2020/6681352>
- [38]. Patel, K., & Patel, D. K. (2024). Biological Potential of Aromadendrin Against Human Disorders: Recent Development in Pharmacological Activities and Analytical Aspects. *Pharmacological Research-Modern Chinese Medicine*, 100424. <https://doi.org/10.1016/j.prmcm.2024.100424>
- [39]. Lopes, I., Campos, C., Medeiros, R., & Cerqueira, F. (2024). Antimicrobial activity of dimeric flavonoids. *Compounds*, 4(2), 214-229. <https://doi.org/10.3390/compounds4020011>
- [40]. Periferakis, A., Periferakis, K., Badarau, I. A., Petran, E. M., Popa, D. C., Caruntu, A., Costache, R. S., Scheau, C., Caruntu, C., & Costache, D. O. (2022). Kaempferol: Antimicrobial Properties, Sources, Clinical, and Traditional Applications. *International journal of molecular sciences*, 23(23), 15054. <https://doi.org/10.3390/ijms232315054>
- [41]. Ye, B., Tian, W., Wang, B., & Liang, J. (2024). CASTpFold: Computed Atlas of Surface Topography of the universe of protein Folds. *Nucleic acids research*, 52(W1), W194-W199. <https://doi.org/10.1093/nar/gkae415>
- [42]. Sayers, E. W., Beck, J., Bolton, E. E., Brister, J. R., Chan, J., Comeau, D. C., Connor, R., DiCuccio, M., Farrell, C. M., Feldgarden, M., Fine, A. M., Funk, K., Hatcher, E., Hoepfner, M., Kane, M., Kannan, S., Katz, K. S., Kelly, C., Klimke, W., Kim, S., ... Sherry, S. T. (2024). Database resources of the National Center for Biotechnology Information. *Nucleic acids research*, 52(D1), D33-D43. <https://doi.org/10.1093/nar/gkad1044>
- [43]. Du, Z., Su, H., Wang, W., Ye, L., Wei, H., Peng, Z., Anishchenko, I., Baker, D., & Yang, J. (2021). The trRosetta server for fast and accurate protein structure prediction. *Nature protocols*, 16(12), 5634-5651. <https://doi.org/10.1038/s41596-021-00628-9>
- [44]. Laskowski, R. A., MacArthur, M. W., Moss, D. S., & Thornton, J. M. (1993). PROCHECK: a program to check the stereochemical quality of protein structures. *Journal of Applied Crystallography*, 26(2), 283-291. <https://doi.org/10.1107/s0021889892009944>
- [45]. Kim, S., Chen, J., Cheng, T., Gindulyte, A., He, J., He, S., Li, Q., Shoemaker, B. A., Thiessen, P. A., Yu, B., Zaslavsky, L., Zhang, J., & Bolton, E. E. (2024). PubChem 2025 update. *Nucleic Acids Research*, 53(D1), D1516-D1525. <https://doi.org/10.1093/nar/gkae1059>
- [46]. Mohanraj, K., Karthikeyan, B. S., Vivek-Ananth, R. P., Chand, R. P. B., Aparna, S. R., Mangalapandi, P., & Samal, A. (2018). IMPPAT: A curated database of Indian Medicinal Plants, Phytochemistry And Therapeutics. *Scientific Reports*, 8(1). <https://doi.org/10.1038/s41598-018-22631-z>
- [47]. Vivek-Ananth, R. P., Mohanraj, K., Sahoo, A. K., & Samal, A. (2023). IMPPAT 2.0: An Enhanced and Expanded Phytochemical Atlas of Indian Medicinal Plants. *ACS Omega*, 8(9), 8827-8845. <https://doi.org/10.1021/acsomega.3c00156>
- [48]. Daina, A., Michielin, O., & Zoete, V. (2014). iLOGP: A Simple, Robust, and Efficient Description of n-Octanol/Water Partition Coefficient for Drug Design Using the GB/SA Approach. *Journal of Chemical Information and Modeling*, 54(12), 3284-3301. <https://doi.org/10.1021/ci500467k>
- [49]. Daina, A., & Zoete, V. (2016). A BOILED-Egg To Predict Gastrointestinal Absorption and Brain Penetration of Small Molecules. *ChemMedChem*, 11(11), 1117-1121. <https://doi.org/10.1002/cmdc.201600182>

Cite this article as: Viknesh Sasikumar and Gopi Uchimuthu., (2025). Computational Exploration of Antifungal plant Compounds as Inhibitors of Squalene Epoxidase in Terbinafine-Resistant *Trichophyton rubrum*, *International Journal of Emerging Knowledge Studies*. 4(1), pp.26-10. <https://doi.org/10.70333/ijeks-03-12-037>